Learning Network Dynamics from Noisy Steady States

1st Yanna Ding
Department of Computer Science
Rensselaer Polytechnic Institute
Troy, United States
dingy6@rpi.edu

2nd Jianxi Gao
Department of Computer Science
Rensselaer Polytechnic Institute
Troy, United States
gaoj8@rpi.edu

3rd Malik Magdon-Ismail
Department of Computer Science
Rensselaer Polytechnic Institute
Troy, United States
magdon@cs.rpi.edu

***Abstract*—We present efficient algorithms to learn the parameters governing the dynamics of networked agents, given equilibrium steady state data. A key feature of our methods is the ability to learn *without seeing the dynamics*, using only the steady states. A key to the efficiency of our approach is the use of mean-field approximations to tune the parameters within a nonlinear least squares (NLS) framework. Our results on real networks demonstrate the accuracy of our approach in two ways. Using the learned parameters, we can: (i) Recover more accurate estimates of the true steady states when the observed steady states are noisy. (ii) Predict evolution to new equilibrium steady states after perturbations to the network topology.**

***Index Terms*—parameter estimation, networked dynamical systems, steady states**

I. Introduction

Understanding the dynamics of networks is crucial in various domains such as ecology [1], [2], epidemiology [3], [4], gene regulatory networks [5], [6], and energy supply networks [7], [8]. Knowing the dynamics also allows one to predict the new equilibrium when networks change. For example whether one species extinction will result in another species extinction [9]. Existing data-driven methods infer dynamics from a time series of observed system-states [10]–[16]. Unfortunately, observing a time-series of states can be costly or impossible. Consider an ecology network in which species interact. The ecological system has evolved over millennia [17], and we only observe the current steady state abundance of each species. We can't collect a time series of species' abundances. Or, consider a biomedical network in which equilibration is at small time scales, making it difficult for experimental devices to capture interim states [18]. Our primary goal is to learn system dynamics when *only* a noisy measurement of the final equilibrium state is available.

The process of learning network dynamics can be time-consuming, especially when it involves repeated numerical integration. One approach to address this is fitting models to the finite difference between time steps, but it may yield inaccurate results with low-resolution data and is not applicable when only the equilibrium state is available. In such cases, the objective function aims to minimize the discrepancy between observed states and those generated by the proposed model using numerical integration techniques [14], [19], [20]. However, numerical integration of network states can be computationally intensive for complex systems with nonlinear and coupled dynamics.

The mean-field network reduction approach, introduced by [21], offers a method to simplify coupled systems while preserving their original dynamics. This approach involves collapsing a high-dimensional network to a one-dimensional representation, facilitating the exploration of the relationship between topology and dynamics. Previous studies have evaluated the accuracy of this approach [21], [22] and extended it to predict steady states from incomplete network topology [23] and infer degrees from observed steady states [24]. Building upon the mean-field approach, our work combines it with nonlinear least squares (NLS) to estimate unknown parameters.

In this study, we propose a surrogate objective function that significantly reduces computational time while approximately preserving the shape of the exact objective function. We approximate parameter-specific steady states using a low-dimensional, decoupled system of ordinary differential equations (ODEs). Through empirical demonstrations, we show that NLS inference using the surrogate objective produces parameters that recover steady states more accurately compared to the observed noisy steady states. Furthermore, our method can predict the new steady states that the system reaches when the network undergoes changes.

II. Method

A. Problem Setup

We work with a universal dynamics framework [25]. The networked system is a graph $\mathcal{G}$, with nodes $\{1, \ldots, N\}$ and adjacency matrix A, where $A_{ij} = 1$ if (i, j) is an edge in $\mathcal{G}$. Suppose the network contains M distinct degrees. We focus on undirected and unweighted graphs. Let δ_i be the degree of

ASONAM '23, November 6–9, 2023, Kusadasi, Turkiye

ACM ISBN 979-8-4007-0409-3/23/11…$15.00
http://dx.doi.org/10.1145/3625007.3631184

Dynamics	$f(\cdot)$	$g(\cdot,\cdot)$
Ecology	$B + x_i\left(1-\frac{x_i}{K}\right)\left(\frac{x_i}{C}-1\right)$	$\frac{x_i x_j}{D+Ex_i+Hx_j}$
Gene regulatory	$-Bx_i^f$	$\frac{x_j^h}{x_j^h+1}$
Epidemic	$-x_i$	$B(1-x_i)x_j$

TABLE I: Summary of the three dynamics analyzed in this paper.

node i. Each node i has a time dependent scalar state $x_i(t)$. The states follow a general form of coupled ODE,

$$\dot{x}_i = f(x_i, \boldsymbol{\theta}) + \sum_{j=1}^{N} A_{ij} g(x_i, x_j, \boldsymbol{\theta}). \tag{1}$$

The functions f and g give the intrinsic and interaction forces. The interaction is modulated by A_{ij}. The functions f, g and the graph topology A are given, while the ODE parameters $\boldsymbol{\theta}$ are unknown and must be learned. We study cooperative dynamics, where $\frac{\partial g}{\partial x_j} \geq 0$ and neighbor's interaction positively affects each component's survival [26]. Since $A_{ij} \geq 0$, nodes with more neighbors have higher equilibria. The three specific dynamics (ecology, gene regulatory, epidemic) which we use in our experiments are summarized in Table I. The nodal state x_i stands for species abundance, gene expression level, and probability of infection in the three dynamics respectively. The ecological dynamics models a plant network projected from plant-pollinator mutualistic relationships. Parameter B, K, C represent the incoming migration rate, carrying capacity, and the Allee constant, respectively [21]. The third term stands for mutualistic interaction that saturate for large x_i, x_j [21], [22]. The gene regulatory dynamics is adapted from the Michaelis-Menten model [6], [27]. The first term denotes degradation ($f = 1$) or dimerization ($f = 2$). The Hill coefficient h represents the level of cooperation of the gene regulation [21], [26]. In the epidemic process, node i is susceptible ($0 \leq x_i < 1$) or infected ($x_i = 1$). Infected nodes spread the pathogen to their neighbors at rate $B \in [0, 1]$ [26].

B. Mean Field Approach

One standard approach to learn the parameters is iterative NLS. Let $\hat{x}_i(\boldsymbol{\theta})$ be the steady states of the system for parameter $\boldsymbol{\theta}$. NLS finds parameters $\boldsymbol{\theta}$ that minimize the error

$$\mathcal{E}(\boldsymbol{\theta}, \mathbf{y}) = \frac{1}{N}\|\hat{\mathbf{x}}(\boldsymbol{\theta}) - \mathbf{y}\|^2 = \frac{1}{N}\sum_{i=1}^{N}(\hat{x}_i(\boldsymbol{\theta}) - y_i)^2. \tag{2}$$

(Boldface is used for vectors and $\|\cdot\|$ is the Euclidean norm.) We define a steady state approximation $\hat{x}_i^{\text{mfa}}(\boldsymbol{\theta}) \approx \hat{x}_i(\boldsymbol{\theta})$ based on a decoupled version of Eq (1) and seek the minimizer of the following surrogate objective function

$$\mathcal{E}^{\text{mfa}}(\boldsymbol{\theta}, \mathbf{y}) = \frac{1}{N}\sum_{i=1}^{N}(\hat{x}_i^{\text{mfa}}(\boldsymbol{\theta}) - y_i)^2. \tag{3}$$

The derivation of $\hat{x}_i^{\text{mfa}}$ uses a reduction of the N-dimensional ODEs (Eq (1)) to a 1-dimensional mean-field equation described in [21]. We summarize the reduction process as follows. The derivation holds for any feasible parameter and we temporarily drop the dependence on $\boldsymbol{\theta}$.

In a network with low degree correlation, the neighborhoods of different nodes exhibit similarities. We assume that the impact received from these neighborhoods is identical for all nodes and consider the shared neighbor effect as a sum of interaction terms weighted by the relative degree of each individual node. We approximate the local neighborhood impact $\sum_{j=1}^{N} A_{ij} g(x_i, x_j)$ by the following shared global impact:

$$\sum_{j=1}^{N} \frac{\delta_j}{\sum_k \delta_k} g(x_i, x_j) \tag{4}$$

Note that Equation 4 is independent of A_{ij}, which is the specific incoming connections to i. The definition of the global state is reasonable because in connected graphs, each node's information propagates throughout the entire network, influencing every node. Furthermore, nodes with larger degrees have a higher impact on other nodes.

To simplify notation, we introduce an averaging linear operator $\mathcal{L} : \mathbb{R}^N \to \mathbb{R}$, which maps a vector $\mathbf{x}$ in $\mathbb{R}^N$ to a scalar:

$$\mathcal{L}(\mathbf{x}) = \frac{\mathbf{1}^\top A \mathbf{x}}{\mathbf{1}^\top A \mathbf{1}} = \sum_{j=1}^{N} \frac{\delta_j x_j}{\sum_k \delta_k} \tag{5}$$

where $\mathbf{1}$ is a vector consisting of all ones. By replacing the local averaging of neighbor effects with the global impact, we obtain:

$$\dot{x}_i \approx f(x_i) + \delta_i \mathcal{L}(g(x_i, \mathbf{x})) \tag{6}$$

where $g(x_i, \mathbf{x}) = [g(x_i, x_1), \ldots, g(x_i, x_N)]$. We further approximate the term $\mathcal{L}(g(x_i, \mathbf{x}))$ by $g(x_i, \mathcal{L}(\mathbf{x}))$:

$$\dot{x}_i \approx f(x_i) + \delta_i g(x_i, \mathcal{L}(\mathbf{x})). \tag{7}$$

This approximation is exact when $g(x_i, x_j)$ is linear in x_j. In vector form, this system is

$$\dot{\mathbf{x}} \approx f(\mathbf{x}) + \boldsymbol{\delta} \circ g(\mathbf{x}, \mathcal{L}(\mathbf{x})). \tag{8}$$

where $f(\mathbf{x}) = [f(x_1), \ldots, f(x_N)]$, $g(\mathbf{x}, \cdot) = [g(x_1, \cdot), \ldots, g(x_N, \cdot)]$, and $\circ$ denotes entrywise product between vectors. Applying $\mathcal{L}$ on both sides reduces this system to one dimension,

$$\mathcal{L}(\dot{\mathbf{x}}) \approx \mathcal{L}[f(\mathbf{x})] + \mathcal{L}[\boldsymbol{\delta} \circ g(\mathbf{x}, \mathcal{L}(\mathbf{x}))]. \tag{9}$$

Since $\mathcal{L}$ is linear, $\mathcal{L}(\dot{\mathbf{x}}) = \mathcal{L}(\dot{\mathbf{x}})$. The following approximation assumes f, g are linear and $\mathcal{L}$ roughly preserves multiplication.

$$\mathcal{L}(\dot{\mathbf{x}}) \approx f(\mathcal{L}(\mathbf{x})) + \mathcal{L}(\boldsymbol{\delta}) g(\mathcal{L}(\mathbf{x}), \mathcal{L}(\mathbf{x})). \tag{10}$$

Define a global effective state $x_{\text{eff}} = \mathcal{L}(\mathbf{x})$ and an effective scalar representation of topology $\beta = \mathcal{L}(\boldsymbol{\delta})$. Then, from Eq (10), x_{eff} approximately follows the dynamics

$$\dot{x_{\text{eff}}} = f(x_{\text{eff}}) + \beta g(x_{\text{eff}}, x_{\text{eff}}). \tag{11}$$

Using x_{eff} for $\mathcal{L}(\mathbf{x})$ in Eq (7), we get the uncoupled ODE for

x_i:

$$\dot{x}_i = f(x_i) + \delta_i g(x_i, x_{\text{eff}}). \tag{12}$$

To compute the steady states $\hat{\mathbf{x}}(\boldsymbol{\theta})$ at an arbitrary parameter $\boldsymbol{\theta}$, there are three steps. (i) Integrate the 1-dimensional ODE (Eq (11)) with initial condition $\mathcal{L}(\mathbf{y})$ to get $\hat{x}_{\text{eff}}$. This biases $\hat{x}_{\text{eff}}$ toward the "right" zero of $f(x, \boldsymbol{\theta}) + \beta g(x, x, \boldsymbol{\theta})$. (ii) Solve the uncoupled ODEs in Eq (12) with initial condition $\hat{x}_{\text{eff}}$. Let z_i denote the ultimate state value. (iii) Perform k numerical integration steps on the full coupled ODEs (Eq (1)) with initial condition z_i to fine tune the mean-field steady states. When no fine-tuning steps are performed in step (iii) ($k = 0$), we get our *mfa* method, which is not only extremely efficient, but only requires node-degrees and not full topology to estimate the parameters, since the scalar topology β can be written as:

$$\beta = \frac{\mathbf{1}^\top A \boldsymbol{\delta}}{\mathbf{1}^\top A \mathbf{1}} = \frac{\boldsymbol{\delta}^\top \boldsymbol{\delta}}{\boldsymbol{\delta}^\top \mathbf{1}} \tag{13}$$

Note that in *mfa*, one only needs to solve Eq (12) for each distinct node-degree, which reduces the system dimension to M (M equals the number of unique degrees). An enhanced method *mfa+* ($k > 0$ in step (iii)) starts from the output of *mfa* and simulates the exact ODEs (Eq (1)) to get more accurate steady states. We refer to solving the original coupled ODE from the given initial condition $\mathbf{x}(0)$ as the *full* algorithm. Our empirical findings demonstrate that leveraging the mean-field approximation significantly enhances the efficiency of parameter estimation from steady states.

III. Empirical Evaluation

We evaluate the learned parameters based on their ability to reproduce the noiseless ground truth steady states $\mathbf{x}^*$. This choice is motivated by two factors. First, in the case of noiseless data, reproducing the steady states is equivalent to reproducing the ground truth parameters. Second, when the observed data is noisy, the minimizer deviates from the ground truth parameter. Therefore, we prioritize the reproduction of noiseless steady states in evaluating the learned parameters. To make a standardized comparison across different networks with varying steady state ranges, we use the mean relative error $\langle |(\hat{\mathbf{x}}(\hat{\boldsymbol{\theta}}) - \mathbf{x}^*)/\mathbf{x}^*| \rangle$, where $\langle \cdot \rangle$ represents the mean of the elements in the enclosed vector.

We use the same ground truth parameters and initial conditions as in previous studies [21], [23]. For ecological networks, the true parameters are set to $B = 0.1, K = 5, C = 1, D = 5, E = 0.9, H = 0.1$. The true parameters for gene regulatory networks are $B = f = 1, h = 2$, and for epidemic networks, $B = 0.5$. The initial conditions of the states are $\forall\ i \in \mathcal{V},\ x_i = 6$ for ecological and gene regulatory dynamics and $\forall\ i \in \mathcal{V},\ x_i = 0.5$ for epidemic networks.

Table II lists the network data used in our experiments. The networks include two mutualistic networks (Net8,Net6) [21], two transcription networks of Saccharomyces cerevisiae (TYA,MEC) [21], a human contact network (Dublin) [28], and an email communication network (Email) [29], [30]. We analyze two types of synthetic networks: Erdős-Rényi (ER) and scale-free (SF). Their degree distribution follow Poisson and power distribution respectively. We use SciPy's ODEINT [31] to numerically integrate ODEs and compute steady states. We consider a simulated state $\hat{\mathbf{x}}(\boldsymbol{\theta})$ as the network equilibrium under parameter $\boldsymbol{\theta}$ if $\langle |d\hat{\mathbf{x}}(\boldsymbol{\theta})/dt| \rangle < 10^{-8}$.

TABLE II: The real network data analyzed in the paper. For each network, we show its number of nodes and edges, dynamics, and the mean ($\langle \mathbf{x}^* \rangle$) and standard deviation (σ) of the ground truth steady states.

Net	Dynamics	# nodes	# edges	$\langle \mathbf{x}^* \rangle \pm \sigma$
Net8	Ecology	97	972	11.4 ± 2.7
Net6	Ecology	270	8074	9.5 ± 0.74
TYA	Regulatory	662	1062	2.8 ± 4.3
MEC	Regulatory	2268	5620	11.48 ± 3.36
Dublin	Epidemic	410	2765	0.78 ± 0.14
Email	Epidemic	1133	5451	0.82 ± 0.05

A. Efficiency

We compare the performance of two variants of our method and the *full* algorithm using real networks in Table III. We generate observations from a normal distribution with a mean x_i^* and a standard deviation $0.1|x_i^*|$. When the initial parameter guess was randomly sampled from a uniform distribution, our *mfa* method demonstrated superior efficiency compared to the other approaches, while maintaining a small loss of accuracy for ecological and epidemic networks. Furthermore, our enhanced variant, *mfa+*, achieved comparable accuracy to the *full* algorithm in a slightly shorter time frame. In cases where the initial parameter guess was sampled from a normal distribution $\mathcal{N}(\boldsymbol{\theta}^*, 0.2\boldsymbol{\theta}^*)$, both *mfa* and *mfa+* exhibited significantly improved speed over the *full* algorithm, with *mfa+*, maintaining the same quality as *full* in reproducing ground truth steady states. When applied to ecological networks, optimizing the *full* objective with the initial parameter guess obtained from *mfa* achieves the same performance as directly optimizing the *full* objective, but in half the time.

The accuracy of the mean-field objective function approximation relies on the dynamics and topology of the system. Specifically, the surrogate objective function effectively captures the exact objective for networks characterized by linear dynamics and homogeneous degree distributions. Consequently, the relative steady-state error is lower for ecological and epidemic networks compared to gene regulatory networks.

Additionally, we study the capability of the learned parameters to recover steady states after topology changes. We randomly rewire 10% edges to obtain new network topology and assume the new network is governed by the same ground truth parameters $\boldsymbol{\theta}^*$. Fig. 1 shows that the parameters learned using noisy steady states of the old network can predict the new equilibria.

TABLE III: This table shows the runtime and relative steady-state error of parameters learned through three different methods to compute steady states in the objective function. We sample initial parameter guess from a distribution $P(\boldsymbol{\theta}^{(0)})$, either uniform or normal. Distribution $\mathcal{N}$ stands for $\mathcal{N}(\boldsymbol{\theta}^*, 0.2\boldsymbol{\theta}^*)$.

Net	$P(\boldsymbol{\theta}^{(0)})$	Runtime (s)			Relative error (%)		
		full	*mfa+*	*mfa*	*full*	*mfa+*	*mfa*
Net8	$U[0,10]$	267	221	29	2.4	2.4	2.5
	$\mathcal{N}$	289	2	10	1.9	1.9	2.1
Net6	$U[0,10]$	8558	6516	107	1.6	1.6	2.4
	$\mathcal{N}$	5257	34	23	1.8	1.8	2.2
TYA	$U[0,3]$	369	373	67	3.3	3.6	9.8
	$\mathcal{N}$	210	165	29	3.7	3.7	6.8
MEC	$U[0,3]$	2456	1161	97	5	6.7	12.9
	$\mathcal{N}$	1656	993	82	4.7	4.7	6.2
Dublin	$U[0,1]$	4	1	0.5	0.5	0.5	2.5
	$\mathcal{N}$	3	0.9	0.4	0.5	0.5	2.5
Email	$U[0,1]$	19	6	0.6	0.34	0.34	3.9
	$\mathcal{N}$	16	1.2	0.5	0.34	0.34	3.9

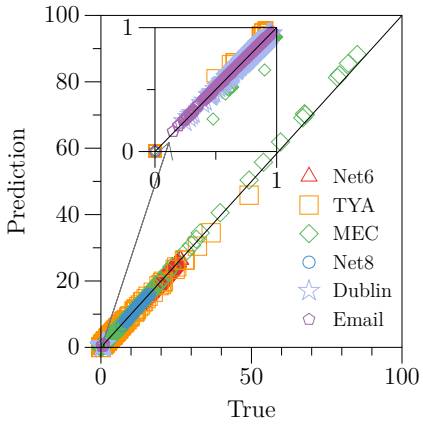

Fig. 1: Predicting steady state using learned parameters compared to true steady state after rewiring 10% of the edges. The prediction determined by $\hat{\boldsymbol{\theta}}$ approaches ground truth steady state computed using $\boldsymbol{\theta}^*$ on the perturbed topology.

B. Denoising Observed Steady States

We assess the performance of our methods under various types and levels of data distortion. Specifically, we consider Gaussian noise, where the observations are generated according to $y_i \sim \mathcal{N}(x_i^*, \epsilon|x_i^*|)$ ($\epsilon \in [0, 0.3]$). We evaluate the effectiveness of the *mfa* method on ER and SF networks. For ER networks, we observe that the predicted state error remains smaller than the observation error even as the noise level increases from 0 to 30%. However, for scale-free networks, the steady state error is reduced compared to the observation error only when the noise level exceeds 3% (see Fig. 2). In cases where the noise level is minimal and the network is heterogeneous, the parameters learned from *mfa* may require fine-tuning using an enhanced version such as *mfa+*. It is worth noting that despite the presence of Gaussian noise, the approximation of the minima of the surrogate surface to the exact error surface remains largely unaffected, indicating a robust alignment between the two surfaces.

We simulate mismeasuring of data by setting 5% of nodes to zero and adding Gaussian-distributed noise $\mathcal{N}(0, 13\%x_i^*)$ to other nodes. The NLS with *mfa* restores the states of the contaminated nodes. The vanishing states are recovered, and the relative state error is reduced from 16% to 5%. The result guides a second round of learning by signifying the mismeasured nodes whose measurement differs drastically from prediction. We identify such nodes as the set $\mathcal{V}' = \{i \in \mathcal{V} : |(y_i - \hat{x}_i)/(y_i + 10^{-8})| \geq 1\}$. We discard the nodes in $\mathcal{V}'$ and optimize the following objective $\sum_{i \notin \mathcal{V}'}(\hat{x}_i(\boldsymbol{\theta}) - y_i)^2$. The second round of learning lowers the state error to 2%.

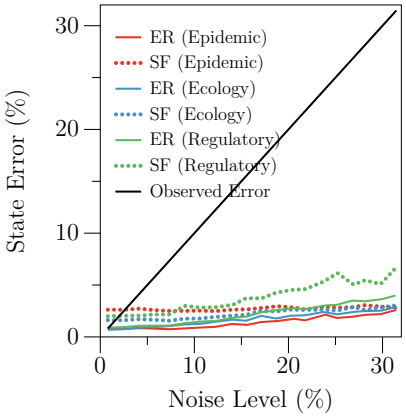

Fig. 2: The relative steady-state prediction error is evaluated for synthetic networks under Gaussian noise. The black line represents the observation error caused by the noise. The solid lines correspond to an ER network with 200 nodes and 811 edges, while the dotted lines correspond to a scale-free network with 200 nodes and 784 edges. We minimize the mean-field objective function using an initial parameter guess sampled from $\mathcal{N}(\boldsymbol{\theta}^*, 20\%|\boldsymbol{\theta}^*|)$. Despite the increasing error in the observed equilibrium, the learned parameter yields states that closely approximate the ground truth steady states.

C. Topology's Role in Learning Parameters

We investigate the contribution of heterogeneity of degrees and number of nodes with the same degree to the denoising effect for BRNs and ER models. The performance is measured using an improvement in steady-state reconstruction

$$\text{Improvement} = \frac{(\text{MSE}(\mathbf{y}) - \text{MSE}(\hat{\mathbf{x}}))}{\text{MSE}(\hat{\mathbf{x}})} \tag{14}$$

where $\hat{\mathbf{x}}$ is the steady state simulated by the learned parameter $\hat{\boldsymbol{\theta}}$ and $\text{MSE}(\mathbf{x})$ is the mean squared error of $\mathbf{x}$ in approximating the true states $\mathbf{x}^*$. The improvement ranges from -1 to ∞. If the value is in $[-1, 0]$, the estimation is worse than the observation. A greater value reflects a larger denoising effect. Fig. 3 shows that learned parameters offer a greater improvement for more homogeneous networks. In particular, ER networks with higher density or SF networks with smaller power-law exponents are more homogeneous and have an overall larger improvement.

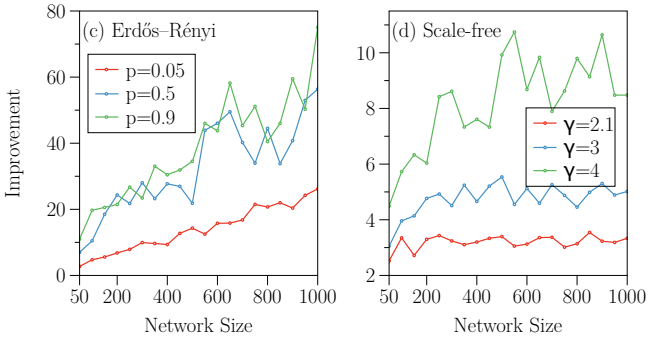

Fig. 3: We use ecological dynamics as an example to investigate the influence of network topology on the accuracy of learned parameters. We sample network sizes from the range of $[50, 1000]$ and vary the density $p = \langle \boldsymbol{\delta} \rangle / (N-1)$ for ER networks and the power distribution coefficient γ for SF networks. For each network, we learn a parameter from noisy steady states (with 10% noise level) using NLS with *mfa*.

IV. Conclusion

We presented an NLS framework learning dynamics in complex systems. Our mean-field approach empirically achieves much faster speed while preserving accuracy. We demonstrated that the learned dynamics *denoises* erroneous observations. By enforcing consistency between observed steady states and learned dynamics, we can rectify significant mismeasurements. This denoising feature has practical applications, such as correcting ecological network species measurements or sentiment reports in social networks. Additionally, the learned parameters are also able to accurately predict the new final equilibrium if the network undergoes topology changes. Our current work leveraged prior knowledge of function forms and topology. For future directions, our goal is to extend our approach to efficiently infer network dynamics without the need for such prior information. Simultaneously, we aim to improve the method's performance on networks with heterogeneous degree distributions.

V. Acknowledgments

We acknowledge the support of National Science Foundation under Grant No. 2047488.

References

[1] J. N. Holland, D. L. DeAngelis, and J. L. Bronstein, "Population dynamics and mutualism: functional responses of benefits and costs," *The American Naturalist*, vol. 159, no. 3, pp. 231–244, 2002.

[2] P. Landi, H. O. Minoarivelo, Å. Brännström, C. Hui, and U. Dieckmann, "Complexity and stability of ecological networks: a review of the theory," *Population Ecology*, vol. 60, pp. 319–345, 2018.

[3] W.-m. Liu, H. W. Hethcote, and S. A. Levin, "Dynamical behavior of epidemiological models with nonlinear incidence rates," *Journal of mathematical biology*, vol. 25, pp. 359–380, 1987.

[4] R. Pastor-Satorras, C. Castellano, P. Van Mieghem, and A. Vespignani, "Epidemic processes in complex networks," *Reviews of modern physics*, vol. 87, no. 3, p. 925, 2015.

[5] R. Casey, H. d. Jong, and J.-L. Gouzé, "Piecewise-linear models of genetic regulatory networks: equilibria and their stability," *Journal of mathematical biology*, vol. 52, no. 1, pp. 27–56, 2006.

[6] G. Karlebach and R. Shamir, "Modelling and analysis of gene regulatory networks," *Nature reviews Molecular cell biology*, vol. 9, no. 10, pp. 770–780, 2008.

[7] P. Kessel and H. Glavitsch, "Estimating the voltage stability of a power system," *IEEE Transactions on power delivery*, vol. 1, no. 3, pp. 346–354, 1986.

[8] R. D. Zimmerman, C. E. Murillo-Sánchez, and R. J. Thomas, "Matpower: Steady-state operations, planning, and analysis tools for power systems research and education," *IEEE Transactions on power systems*, vol. 26, no. 1, pp. 12–19, 2010.

[9] F. S. Valdovinos, "Mutualistic networks: moving closer to a predictive theory," *Ecology letters*, vol. 22, no. 9, pp. 1517–1534, 2019.

[10] J. Bongard and H. Lipson, "Automated reverse engineering of nonlinear dynamical systems," *Proceedings of the National Academy of Sciences*, vol. 104, no. 24, pp. 9943–9948, 2007.

[11] S. L. Brunton, J. L. Proctor, and J. N. Kutz, "Discovering governing equations from data by sparse identification of nonlinear dynamical systems," *Proceedings of the national academy of sciences*, vol. 113, no. 15, pp. 3932–3937, 2016.

[12] S. Gugushvili and C. A. Klaassen, "$\sqrt{n}$-consistent parameter estimation for systems of ordinary differential equations: bypassing numerical integration via smoothing," *Bernoulli*, vol. 18, no. 3, pp. 1061–1098, 2012.

[13] E. L. Ionides, C. Bretó, and A. A. King, "Inference for nonlinear dynamical systems," *Proceedings of the National Academy of Sciences*, vol. 103, no. 49, pp. 18 438–18 443, 2006.

[14] J. O. Ramsay, G. Hooker, D. Campbell, and J. Cao, "Parameter estimation for differential equations: a generalized smoothing approach," *Journal of the Royal Statistical Society: Series B (Statistical Methodology)*, vol. 69, no. 5, pp. 741–796, 2007.

[15] M. Schmidt and H. Lipson, "Distilling free-form natural laws from experimental data," *science*, vol. 324, no. 5923, pp. 81–85, 2009.

[16] S. N. Wood, "Statistical inference for noisy nonlinear ecological dynamic systems," *Nature*, vol. 466, no. 7310, pp. 1102–1104, 2010.

[17] L. B. Slobodkin *et al.*, *Growth and regulation of animal populations.* Dover Publications., 1980, no. Ed. 2.

[18] R. Boiger, A. Fiedler, J. Hasenauer, and B. Kaltenbacher, "Continuous analogue to iterative optimization for pde-constrained inverse problems," *Inverse Problems in Science and Engineering*, vol. 27, no. 6, pp. 710–734, 2019.

[19] C. Zang and F. Wang, "Neural dynamics on complex networks," in *Proceedings of the 26th ACM SIGKDD International Conference on Knowledge Discovery & Data Mining*, 2020, pp. 892–902.

[20] Z. Huang, Y. Sun, and W. Wang, "Coupled graph ode for learning interacting system dynamics." in *KDD*, 2021, pp. 705–715.

[21] J. Gao, B. Barzel, and A.-L. Barabási, "Universal resilience patterns in complex networks," *Nature*, vol. 530, no. 7590, pp. 307–312, 2016.

[22] P. Kundu, H. Kori, and N. Masuda, "Accuracy of a one-dimensional reduction of dynamical systems on networks," *Physical Review E*, vol. 105, no. 2, p. 024305, 2022.

[23] C. Jiang, J. Gao, and M. Magdon-Ismail, "True nonlinear dynamics from incomplete networks," in *Proceedings of the AAAI Conference on Artificial Intelligence*, vol. 34, 2020, pp. 131–138.

[24] ——, "Inferring degrees from incomplete networks and nonlinear dynamics," *Proceedings of the Twenty-Ninth International Joint Conference on Artificial Intelligence*, 2020.

[25] B. Barzel and A.-L. Barabási, "Universality in network dynamics," *Nature physics*, vol. 9, no. 10, pp. 673–681, 2013.

[26] R.-J. Wu, Y.-X. Kong, Z. Di, J. Bascompte, and G.-Y. Shi, "Rigorous criteria for the collapse of nonlinear cooperative networks," *Physical Review Letters*, vol. 130, no. 9, p. 097401, 2023.

[27] U. Alon, *An introduction to systems biology: design principles of biological circuits*. Chapman and Hall/CRC, 2006.

[28] R. Rossi and N. Ahmed, "The network data repository with interactive graph analytics and visualization," in *Proceedings of the AAAI conference on artificial intelligence*, vol. 29, 2015.

[29] R. Guimera, L. Danon, A. Diaz-Guilera, F. Giralt, and A. Arenas, "Self-similar community structure in a network of human interactions," *Physical review E*, vol. 68, no. 6, p. 065103, 2003.

[30] J. Kunegis, "Konect: the koblenz network collection," in *Proceedings of the 22nd international conference on world wide web*, 2013, pp. 1343–1350.

[31] P. Virtanen, R. Gommers, T. E. Oliphant, M. Haberland, T. Reddy, D. Cournapeau, E. Burovski, P. Peterson, W. Weckesser, J. Bright *et al.*, "Scipy 1.0: fundamental algorithms for scientific computing in python," *Nature methods*, vol. 17, no. 3, pp. 261–272, 2020.